REPORT DOCUMENTATION PAGE	*Form Approved OMB No. 0704-0188*

1. REPORT DATE *(DD-MM-YYYY)*	2. REPORT TYPE	3. DATES COVERED *(From - To)*
14 Mar 2008	FINAL REPORT	1 Mar 2005 - 31 Oct 2007

4. TITLE AND SUBTITLE

Uniform in time asymptotic and numerical methods for propagation in dielectrics exhibiting fractional relaxation, and efficient and accurate impedance boundary conditions for high-order numerical schemes for the time-dependent maxwell equations

5a. CONTRACT NUMBER FA9550-05-1-0162

5b. GRANT NUMBER 05NM034

5c. PROGRAM ELEMENT NUMBER

5d. PROJECT NUMBER

5e. TASK NUMBER

5f. WORK UNIT NUMBER

6. AUTHOR(S)

Dr. Peter G. Petropoulos
Department of Mathematical Sciences
New Jersey Institute of Technology

7. PERFORMING ORGANIZATION NAME(S) AND ADDRESS(ES)

New Jersey Institute of Technology
University Heights
Newark, NJ 07102

8. PERFORMING ORGANIZATION REPORT NUMBER

9. SPONSORING/MONITORING AGENCY NAME(S) AND ADDRESS(ES)

AF OFFICE OF SCIENTIFIC RESEARCH
875 NORTH RANDOLPH STREET ROOM 3112
ARLINGTON VA 22203
Dr Arje Nachman/NE

10. SPONSOR/MONITOR'S ACRONYM(S)

11. SPONSOR/MONITOR'S REPORT NUMBER(S)

12. DISTRIBUTION/AVAILABILITY STATEMENT

DISTRIBUTION STATEMENT A: UNLIMITED

AFRL-SR-AR-TR-08-0175

13. SUPPLEMENTARY NOTES

14. ABSTRACT

In this paper we examine the small- and large-depth response of a Cole-Cole dielectric half-space subjected to a prescribed incident pulse; the case of delta-function incidence is employed to determine and analyze the resulting impulse response. Our purpose is to contrast our findings to the corresponding ones obtained for the Debye model in order to ascertain whether the time-domain waveforms obtained in a TDR experiment could serve as a means for selecting the most appropriate frequency-domain model for the experimentally obtained dielectric data. Our approach involves both asymptotic and numerical methods. We find that the Cole-Cole model's impulse response is in find that the Cole-Cole model's impulse response is infinitely smooth at the wavefront (small-depth), and determine its shape. It follows that sawtooth and square-pulse waveforms, and all other realistic waveforms, become smooth after travelling a brief time in any Cole-Cole model. This is in contrast to the case of the Debye impulse response which is discontinuous at the wavefront.

15. SUBJECT TERMS

Dielectric models,;Electromagnetic pulse propagation; Time-domain reflectometry

16. SECURITY CLASSIFICATION OF:			17. LIMITATION OF ABSTRACT	18. NUMBER OF PAGES	19a. NAME OF RESPONSIBLE PERSON
a. REPORT	b. ABSTRACT	c. THIS PAGE			19b. TELEPHONE NUMBER *(Include area code)*

Standard Form 298 (Rev. 8/98)
Prescribed by ANSI Std. Z39.18

Uniform in time asymptotic and numerical methods for propagation in dielectrics exhibiting fractional relaxation, and efficient and accurate impedance boundary conditions for high-order numerical schemes for the time-dependent maxwell equations

Peter G. Petropoulos
Department of Mathematical Sciences
New Jersey Institute of Technology
University Heights
Newark, NJ 07102

14 March 2008
Final Report for Period 1 March 2005 - 31 October 2007 (Grant FA9550-05-1-0162)

Prepared for
Air Force Office of Scientific Research/NE
875 North Randolph Road
Ste 325, Room 3112
Arlington, VA 22203

1. Technical Summary of Research Accomplished.

We will first briefly describe the research results that have already been published [1] in the scientific literature, and then we will provide some details of the remaining publications that resulted from the research effort and have been submitted for publication or are still in preparation to be submitted.

1.1. Summary of Published Research Accomplishments.

1.1.1. Introduction. The propagation of short-duration electromagnetic pulses in dielectric media is of interest in diverse technological applications areas such as geophysics (ground-penetrating radar [2]) and bioelectromagnetics (health and safety analyses [3]). Most importantly, time-domain reflectometry (TDR, [4]) employs short-duration electromagnetic pulses in a laboratory setting to obtain the frequency-dependent dielectric properties of materials. Time-domain waveforms of propagated signals in TDR experiments are routinely measured and analyzed [5]-[6]. In the TDR setting, the experimentally determined complex-valued dielectric permittivity $\epsilon(\omega)$ is subsequently fitted to a model assumed to be relevant for the range of frequencies in which measurements are obtained. The two models commonly used to describe the variation of the permittivity with frequency up to about 10 GHz are the Debye [7] and the Cole-Cole [8] models. Examples of the use of the Debye and Cole-Cole models to fit experimentally determined dielectric permittivity data for human tissue include [9] and [10] respectively. The reasons for choosing a particular model to fit a particular set of data are not always clear, e.g., both of the aforementioned models have been used to fit permittivity data obtained for human tissue [10] *and* concrete [11]. A modeled small- and large-depth response of an experimentally examined dielectric subjected to any physically realizable pulse (hence measurable in a TDR experiment) can be obtained by convolution with the appropriate, theoretically obtained, impulse response function; subsequent comparisons to actual response waveforms measured in a TDR setup could be used to determine which model is most appropriate to represent a given set of measured permittivity data.

The response of the Debye dielectric medium model to transient electromagnetic radiation has been investigated in [12]-[14]. These authors found that the wavefront impulse response supports discontinuities on $x = c_\infty t$, where $c_\infty = 1/\sqrt{\epsilon(\infty)\mu_0}$ is the wavefront speed, and that it decays exponentially with depth hence it is important only up to a distance of $O(c_\infty \tau)$ past the air/dielectric interface (the so-called "time-domain skin-depth"). Also [12]-[14], it was found that past that thin layer the impulse response satisfies an advection-diffusion equation, that it travels with the zero-frequency phase speed along the sub-characteristic $x = \frac{c_\infty}{\sqrt{\epsilon_s}} t = c_0 t$, where $\epsilon_s = \epsilon(0)$ is the DC permittivity, and that it diffuses around that sub-characteristic.

In this paper we examine the small- and large-depth response of a Cole-Cole dielectric half-space subjected to a prescribed incident pulse; the case of delta-function incidence is employed to determine and analyze the resulting impulse response. Our purpose is to contrast our findings to the corresponding ones obtained for the Debye model in order to ascertain whether the time-domain waveforms obtained in a TDR experiment could serve as a means for selecting the most appropriate frequency-domain model for the experimentally obtained dielectric data. Our approach involves both asymptotic and numerical methods. We find that the Cole-Cole model's impulse response is infinitely smooth at the wavefront (small-depth), and determine its shape. It follows that sawtooth and square-pulse waveforms, and all other realistic waveforms, become smooth after travelling a brief time in any Cole-Cole model. This is in contrast to the case of the Debye impulse response which is discontinuous at the wavefront. Also, we find that the location of the peak of the main (large-depth) response in the Cole-Cole dielectric model occurs at an earlier space-time location than that found for the Debye dielectric model main response.

1.1.2. Problem Formulation. The dielectric dispersion proposed in [8] defines what is known in the literature as the frequency-domain Cole-Cole dielectric medium model which, in the context of the Laplace transform ($s = i\omega$), takes the form

$$\epsilon(s) = \epsilon_\infty + \frac{\epsilon_s - \epsilon_\infty}{1 + (s\tau)^\alpha}, \tag{1.1}$$

where $0 < \alpha < 1$ is a data-fit parameter, and ϵ_∞, ϵ_s, τ are respectively the infinite-frequency permittivity, the zero-frequency permittivity, and the central relaxation time [15] around which a distribution of relaxation times exists and whose width is controlled by α. The four parameters in (1.1) are fitted to dielectric permittivity data measured over a frequency band, e.g., [10] fits frequency-domain dielectric permittivity data obtained for various biological tissue types to a linear combination of 4 Cole-Cole models. It is known [16] that (1.1) constitutes a causal dielectric model.

For simplicity, we will consider one-dimensional electromagnetic pulse propagation in a homogeneous, non-magnetic ($\mu = \mu_0$, μ_0 is the permeability of vacuum) half-space, $x > 0$, whose frequency-dependent dielectric permittivity is modeled by (1.1). The electric field $E(x,t)$ is prescribed at $x = 0$. The time-dependent Maxwell system reduces to

$$\epsilon_\infty \frac{\partial^2 E}{\partial t^2} + \frac{\partial^2 P}{\partial t^2} = \frac{1}{\mu_0}\frac{\partial^2 E}{\partial x^2}\ ; \quad x > 0, \quad t > 0, \tag{1.2}$$

where $P(x,t)$ is the induced polarization field which describes the response of the dielectric medium to the propagating wave. Using (1.1), the induced polarization is defined as [17]

$$P(x,t) = \int_0^t \chi_\alpha(t-t')E(x,t')dt', \quad t > 0, \tag{1.3}$$

where

$$\chi_\alpha(t) = \mathcal{L}^{-1}\{\frac{\epsilon_s - \epsilon_\infty}{1+(s\tau)^\alpha}\} = \frac{1}{2\pi i}\int_{\zeta - i\infty}^{\zeta + i\infty} \frac{\epsilon_s - \epsilon_\infty}{1+(s\tau)^\alpha} e^{st} ds, \quad t > 0, \tag{1.4}$$

is the Cole-Cole time-domain susceptibility kernel. When $\alpha = 1$, the Debye time-domain susceptibility is obtained. In (1.4), $\mathcal{L}^{-1}$ denotes the inverse Laplace transform performed along the standard Bromwich contour ($Im\{\zeta\} = 0$, $\zeta > 0$) on the complex s-plane cut along the $Re\{s\} < 0$ axis with the branch point at the origin so that $-\pi < arg(s) < \pi$, i.e., the denominator does not introduce any additional singularities in the complex s plane. The initial value $P(x,0) = 0$ is evident from (1.3). The polarization thusly defined also satisfies the fractional-order differential equation

$$\tau^\alpha \frac{d^\alpha P}{dt^\alpha} + P = (\epsilon_s - \epsilon_\infty)E, \quad t > 0; \quad P(x,0) = 0, \tag{1.5}$$

i.e., $\chi_\alpha(t)$ is the Green's function for (1.5) which is obtained when $E = \delta(t)$. The nonlocal-in-time operator $\frac{d^\alpha}{dt^\alpha}$, $0 < \alpha < 1$, denotes the Caputo fractional-order time derivative [18] which, for functions satisfying $P(x,0) = 0$, is defined as

$$\frac{d^\alpha P(x,t)}{dt^\alpha} = \frac{1}{\Gamma(1-\alpha)}\int_0^t \frac{P'(x,u)du}{(t-u)^\alpha}, \tag{1.6}$$

where P' represents differentiation with respect to the time argument of P. Finally, we assume that at $t = 0$ all fields are zero in the half-space $x > 0$, that all fields vanish as $x \to \infty$, $t \geq 0$, and that the electric field is prescribed at $x = 0$, i.e., we consider a signaling problem with boundary data

$$E(0,t) = f(t)\ ; \quad t \geq 0, \tag{1.7}$$

where $f(t)$ is the prescribed electric field.

1.1.3. Asymptotic Analysis for Pulse Propagation. We use the Laplace transform in time to solve (1.2) and (1.5) subject to (1.7), the initial conditions, and the behavior at infinity described in Section

2. After eliminating the P field we determine that for the signaling problem in a Cole-Cole dielectric half space ($x \geq 0$) the electric field is given by the following Bromwich integral

$$E(x,t) = \frac{1}{2\pi i}\int_{\zeta-i\infty}^{\zeta+i\infty} F(s)e^{s[t-\frac{x}{c_\infty}\sqrt{\frac{s^\alpha+\beta}{s^\alpha+\beta\gamma}}]}ds, \quad t \geq \frac{x}{c_\infty}, \tag{1.8}$$

where $-\pi < arg(s) \leq \pi$, $Re\sqrt{\frac{s^\alpha+\beta}{s^\alpha+\beta\gamma}} > 0$, $\beta = \frac{\epsilon_s}{\epsilon_\infty \tau^\alpha}$, $\gamma = \frac{\epsilon_\infty}{\epsilon_s}$, and $F(s) = \mathcal{L}\{f(t)\}$. Closing the Bromwich contour with a semi-circle to the right of $s = \zeta$ we obtain $E(x,t) = 0,\ t < \frac{x}{c_\infty}$, as the integrand exhibits no singularities in that region (causality). For the branch chosen, the square root in (1.8) does not introduce additional singularities (recall $0 < \alpha < 1$) since the argument of the roots of the numerator and denominator is $arg(s) = (\pi + 2k\pi)/\alpha;\ k = 0, \pm 1, ...$, i.e., these roots are outside the chosen principal branch.

We next consider (1.8) for $t \to \frac{x^+}{c_\infty}$, i.e., for times immediately after the arrival of the wavefront described by the characteristic ray $x = c_\infty t$ at a fixed x location, and for $t \approx \frac{x}{c_\infty} \gg 1$.

The Wavefront Region ($t \to \frac{x^+}{c_\infty}$)

A large$-s$ expansion of the bracketed expression in (1.8)

$$(t - \frac{x}{c_\infty}) + \frac{x}{c_\infty}(1 - \sqrt{\frac{s^\alpha+\beta}{s^\alpha+\beta\gamma}}) = (t - \frac{x}{c_\infty}) - \frac{x}{c_\infty}\frac{\beta(1-\gamma)}{2}s^{-\alpha} + O(s^{-2\alpha}) \tag{1.9}$$

results in

$$E(x,t) = \frac{1}{2\pi i}\int_{\zeta-i\infty}^{\zeta+i\infty} F(s)e^{-As^{1-\alpha}}(1 + O(s^{1-2\alpha}))e^{s(t-\frac{x}{c_\infty})}ds, \tag{1.10}$$

where $A = \frac{x}{c_\infty}\frac{\beta(1-\gamma)}{2} > 0$. Due to $0 < 1-\alpha < 1$, we determine that

$$\lim_{t \to \frac{x^+}{c_\infty}} \frac{d^n}{dt^n}E(x,t) = 0,\ n \geq 0,$$

since

$$\lim_{s\to\infty} s^n F(s)(1 + O(s^{1-2\alpha}))e^{-As^{1-\alpha}} = 0,\ n \geq 0.$$

Thus, the impulse response of the Cole-Cole medium is infinitely smooth at the wavefront even in the case of $F(s) = 1$ ($f(t) = \delta(t)$ signaling data). In contrast, setting $\alpha = 1$ (Debye model) in (1.10) we obtain

$$E(x,t) \approx e^{-\frac{x}{2c_\infty\tau}(\frac{\epsilon_s}{\epsilon_\infty}-1)}f(t - \frac{x}{c_\infty}), \tag{1.11}$$

i.e., the Debye wavefront impulse response inherits the continuity properties of $f(t)$ at $t = 0$ [13].

For the special case $\alpha = 1/2$, standard Laplace transform tables allow us to invert the leading-order term in (1.10) via

$$\mathcal{L}^{-1}\{e^{-\frac{x}{c_\infty}\frac{\beta(1-\gamma)}{2}s^{1/2}}\} = \frac{1}{4\sqrt{\pi}}\frac{\beta(1-\gamma)}{c_\infty}\frac{x}{t^{3/2}}e^{-\frac{\beta^2(1-\gamma)^2x^2}{16c_\infty^2 t}}, \quad t > 0, \tag{1.12}$$

and obtain the approximate short-time response

$$E(x,t) \approx \frac{1}{4\sqrt{\pi}}\frac{\beta(1-\gamma)}{c_\infty}x\int_{x/c_\infty}^{t} f(t-\xi)\frac{1}{(\xi - x/c_\infty)^{3/2}}e^{-\frac{\beta^2(1-\gamma)^2x^2}{16c_\infty^2(\xi - x/c_\infty)}}d\xi. \tag{1.13}$$

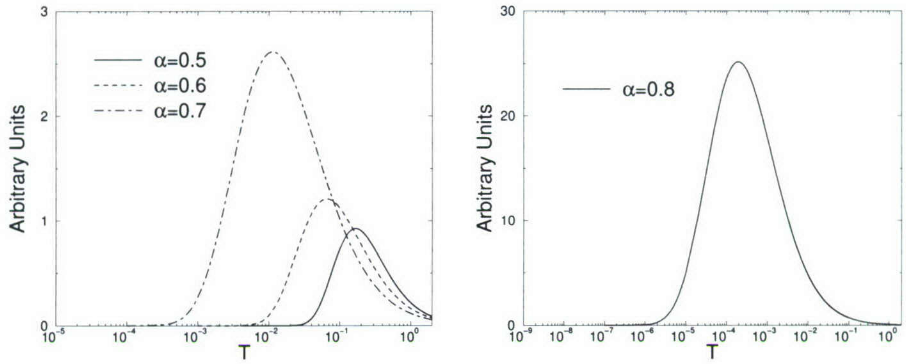

(a) (b)

FIG. 1.1. *Wavefront response for $\delta(t)$ signaling data and $0.5 \leq \alpha \leq 0.8$; $T = t - \frac{x}{c_\infty}$.*

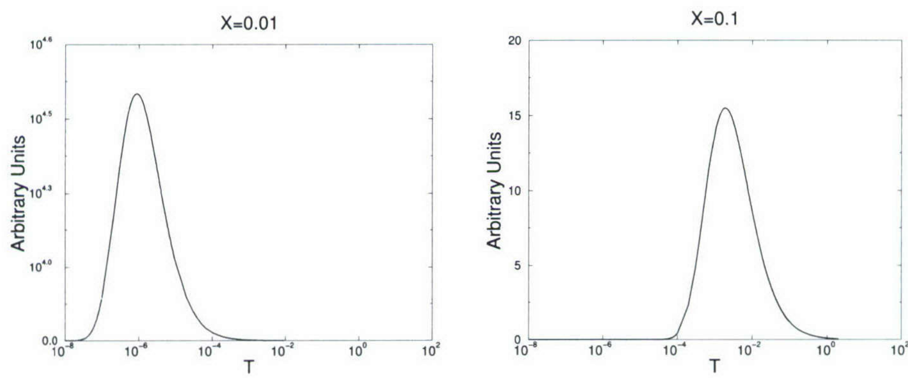

(a) (b)

FIG. 1.2. *The wavefront impulse response (1.15) at two depths for $\alpha = 0.7$.*

For other values of α we proceed by collapsing the Bromwich contour in (1.10) onto the branch cut defined earlier and employing the change of integration variable $s = re^{\pm i\pi}$ to calculate the function $\Psi_\alpha(t) = \mathcal{L}^{-1}\{e^{-s^{1-\alpha}}\},\ t > 0$, where

$$\Psi_\alpha(t) = \frac{1}{\pi}\int_0^\infty e^{-tr}e^{-r^{1-\alpha}\cos[\pi(1-\alpha)]}\sin(r^{1-\alpha}\sin[\pi(1-\alpha)])dr. \tag{1.14}$$

Then, using (1.14), a change of variables $s' = A^{\frac{1}{1-\alpha}}s$ in (1.10) and subsequent dropping of the prime, and the translation theorem we can write an integral expression for the approximate wavefront response (1.10) for any $0 < \alpha < 1$ as a convolution of $f(t)$ with the approximate impulse response function

$$\mathcal{I}^{app}(x,t) = \mathcal{L}^{-1}\{e^{-As^{1-\alpha}}\} = A^{-\frac{1}{1-\alpha}}\Psi_\alpha(A^{-\frac{1}{1-\alpha}}(t - \frac{x}{c_\infty})),\quad t \geq \frac{x}{c_\infty}. \tag{1.15}$$

For demonstration purposes we employed Mathematica to evaluate the integral in (1.14) for $0 < T = t - \frac{x}{c_\infty} < 2$; Figure 1.1 shows the wavefront impulse response for medium parameters and depth such that $A = 1$ and various values of α; as $\alpha \to 1^-$ the right hand side of (1.14) approaches a delta function in time

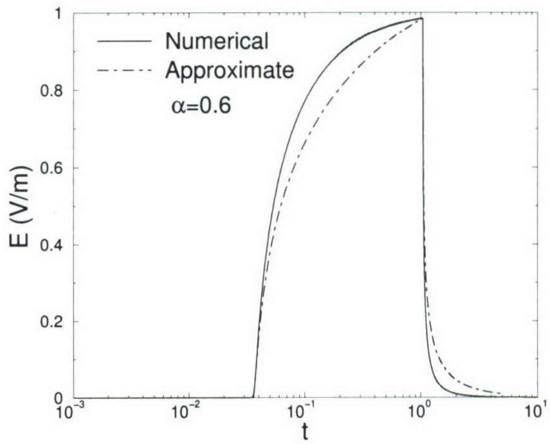

FIG. 1.3. *Comparison of approximate response near the wavefront to a numerical solution of the full problem;* $\frac{x}{c_\infty \tau} = 0.036$.

and the numerical evaluation of the integral fails. We note that in the case of unit step-function signaling data ($F(s) = 1/s$) the approximate wavefront response exhibits self-similarity, i.e, $E(x,t) = \Phi_\alpha(\xi)$, where $\xi = A^{-\frac{1}{1-\alpha}}(t - \frac{x}{c_\infty})$ is the similarity variable, and $\Phi_\alpha(\xi) = \int_0^\xi A^{-\frac{1}{1-\alpha}} \Psi_\alpha(A^{-\frac{1}{1-\alpha}} t)dt$, where we have used $\Psi_\alpha(0) = 0$ and the integration property of the Laplace transform. Figure 1.2 shows the dependence of $\mathcal{I}^{app}(x,t)$ on the depth x (effected by varying A) for $\alpha = 0.7$ and representative medium parameters; the rapidly diminishing vertical scale indicates the rapid decay of the wavefront response. We also note that the peak of the response behind the wavefront $T = 0$ is delayed by an amount that depends on both α and x (see Figures 1.1-1.2). We have verified the results shown in Figures 1.1-1.2 by using Mathematica to evaluate the following alternative representation of $\Psi_\alpha(t)$ [19],

$$\Psi_\alpha(t) = \sum_{k=1}^{\infty} (-1)^{k-1} \frac{t^{-(1-\alpha)k-1}}{\Gamma(1+k)\Gamma(k(\alpha-1))}. \tag{1.16}$$

Figure 1.3 shows a validation of the approximate response obtained at $x = 0.036 c_\infty \tau$ by convolving (1.15), for $\alpha = 0.6$, with a rectangular pulse function $f(t)$ of duration τ seconds. The numerical result (solid line) is a solution of the full problem consisting of (1.2) and (1.5) using a novel technique we developed in [20] for computing the fractional derivative (1.6) with a known, *a priori* set, error that is uniform in time.

The $t \approx \frac{x}{c_\infty} \gg 1$ Region

To obtain the large-depth impulse response we evaluate (1.8) for the case $F(s) = 1$ using the saddle-point method. We first rewrite (1.8) as

$$E(x,t) = \frac{1}{2\pi i} \int_{\zeta - i\infty}^{\zeta + i\infty} e^{\lambda Q(s,\theta)} ds, \tag{1.17}$$

where $\theta = \frac{c_\infty t}{x} \geq 1$ is the space-time parameter, $Q(s,\theta) = s[\theta - \sqrt{\frac{s^\alpha + \beta}{s^\alpha + \beta\gamma}}]$, and $\lambda = x/c_\infty$ is the large parameter. We obtain the location of the saddle points $\bar{s}$ by setting $\frac{\partial Q(s,\theta)}{\partial s} = 0$ and solving for $s = \bar{s}$. The following equation holds for the saddle points:

$$\theta = \sqrt{\frac{s^\alpha + \beta}{s^\alpha + \beta\gamma}} [1 - \frac{\alpha\beta/2}{s^\alpha + \beta} + \frac{\alpha\beta\gamma/2}{s^\alpha + \beta\gamma}]. \tag{1.18}$$

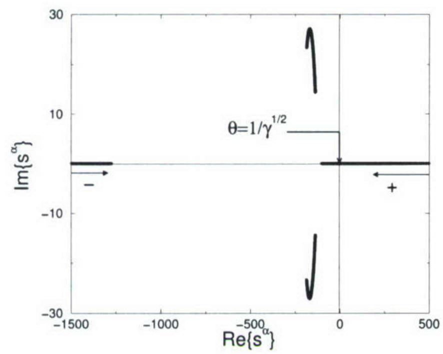

FIG. 1.4. *Motion of the roots of (1.18) for* $1 < \theta \leq \frac{5}{\sqrt{\gamma}}$ *and* $\alpha = 0.7$.

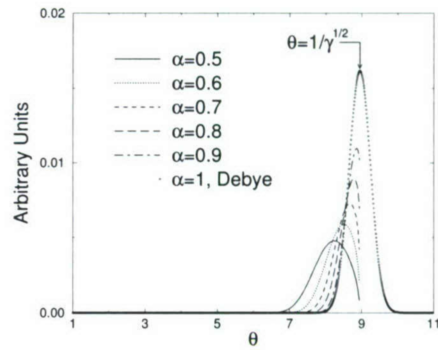

FIG. 1.5. *Leading order asymptotic response at* $x/c_\infty =$ *100 as a function of* α.

By rationalizing (1.18) we obtain a fourth order polynomial in s^α whose roots we find numerically for a representative set of parameters. A typical root portrait is shown in Figure 1.4; the arrows indicate the direction of motion of the real roots. As θ increases from 1, the single positive real root s^α decreases from ∞ and moves towards $s = 0$ (the arrow labelled with the positive sign). The arrow labelled with the negative sign indicates the direction of motion of the negative real root as θ varies. When $\theta = 1/\sqrt{\gamma} = c_\infty/c_0$ (as indicated on the Figure), the real root is $s^\alpha = 0$. For $\theta > c_\infty/c_0$ both real roots of (1.18) are negative. The complex roots of (1.18) always lie in the second and third quadrants. Consequently, on the principal sheet defined by the branch cut introduced earlier by s^α, only the positive real root of (1.18) survives to provide a saddle point. Thus, for each value of $1 \leq \theta < c_\infty/c_0$ there corresponds one saddle point $\infty > \bar{s} > 0$ on the real $s-$axis. For $\theta \geq c_\infty/c_0$ the saddle point first coalesces with the branch point at the origin and then moves into the branch cut. Consequently, the Bromwich contour is no longer equivalent to a steepest descent contour. In the region $1 < \theta < c_\infty/c_0$ we can apply the saddle point method using $\lambda = x/c_\infty$ as our large parameter. A small$-s$ expansion of $Q(s, \theta)$,

$$Q(s,\theta) \approx s(\theta - \frac{1}{\sqrt{\gamma}} + \frac{1-\gamma}{2\beta\gamma^{3/2}} s^\alpha), \tag{1.19}$$

allows us to obtain an approximation to the saddle point, i.e.,

$$\bar{s} = B^{\frac{1}{\alpha}} (\frac{1}{\sqrt{\gamma}} - \theta)^{\frac{1}{\alpha}}, \tag{1.20}$$

where $B = \frac{2\beta\gamma^{3/2}}{(1-\gamma)(1+\alpha)}$. We find that $\frac{\partial^2 Q(s,\theta)}{\partial s^2}|_{s=\bar{s}} = \alpha B^{-\frac{1}{\alpha}} (\frac{1}{\sqrt{\gamma}} - \theta)^{1-\frac{1}{\alpha}} > 0$ hence the local steepest descent directions at $\bar{s}$ are $arg(s - \bar{s}) = \frac{\pi}{2}, \frac{3\pi}{2}$. We obtain the result

$$E(x,t) \approx \frac{e^{\lambda Q(\bar{s},\theta)}}{\sqrt{2\pi\lambda Q_{ss}(\bar{s},\theta)}} \times [1 + \frac{(1-\alpha)(1+2\alpha)}{24\alpha\lambda B^{1/\alpha}(\frac{1}{\sqrt{\gamma}} - \theta)^{1+\frac{1}{\alpha}}}]. \tag{1.21}$$

In Figure 1.5 we plot the leading order term of (1.21) as a function of θ for various α, and note that its peak does not occur on the sub-characteristic ray, $x = c_0 t$ ($\theta = \frac{1}{\sqrt{\gamma}}$), as it does in the case of the Debye medium ($\alpha = 1$) [12]-[13]. Rather, the peak of the response arrives earlier, at a $\theta < \frac{1}{\sqrt{\gamma}}$, and its space-time location now depends on α. Also, we notice that the leading-order result breaks down, i.e., $E(x,t) = 0$, for $\theta = \frac{1}{\sqrt{\gamma}}$ and $0 < \alpha < 1$; the second term in (1.21), the correction, diverges at $\theta = \frac{1}{\sqrt{\gamma}}$ since the derivation of (1.21)

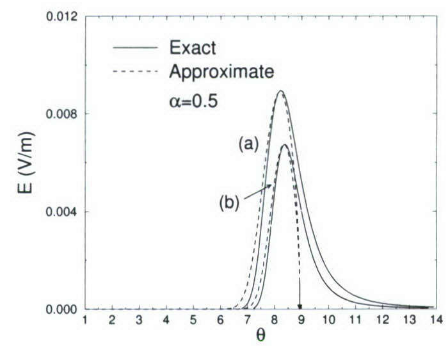

FIG. 1.6. *Comparison of Equation (1.21) and (1.17) for (a) $x/c_\infty = 50$, (b) $x/c_\infty = 100$. The arrow indicates the location of the peak of the response for $\alpha = 1$.*

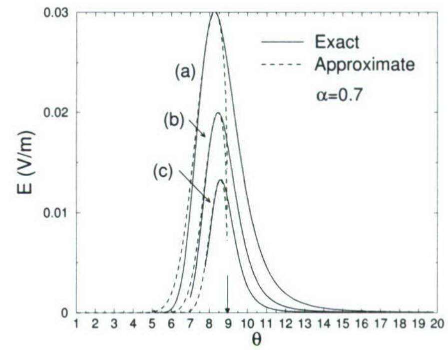

FIG. 1.7. *Comparison of Equation (1.21) and (1.17) for (a) $x/c_\infty = 10$, (b) $x/c_\infty = 20$, (c) $x/c_\infty = 40$. . The arrow indicates the location of the peak of the response for $\alpha = 1$.*

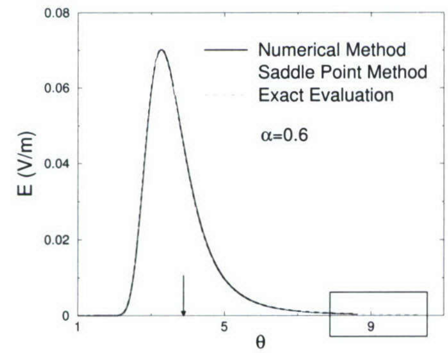

FIG. 1.8. *Comparison of Equation (1.21) and (1.17) with a numerical simulation [20] for $x/c_\infty = 9.216$. The arrow indicates the location of the peak of the response for $\alpha = 1$.*

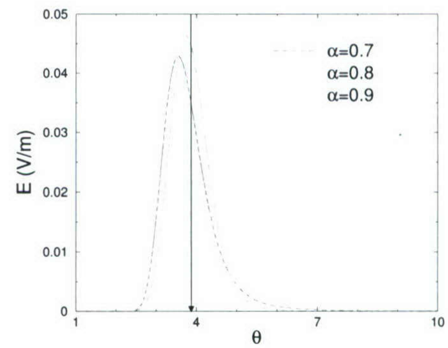

FIG. 1.9. *Large-depth response for $x/c_\infty = 18.432$; both peak location and value depend on α. The arrow indicates the location of the peak of the response for $\alpha = 1$.*

does not take into account the coalescence of the saddle point with the branch point at $s = 0$. Despite this failure, the result is useful; Figures 1.6-1.7 show a comparison between the leading order sadle-point method result, and an evaluation of (1.17) for various values of α and x/c_∞ using Mathematica. The Mathematica results have been verified using the numerical technique developed in [20]; Figure 1.8 shows such a verification where the numerical result overlaps the Mathematica evaluation of (1.17), as indicated by the boxed region, and both results agree with the approximate response peak location. We note that Figures 1.6-1.8 indicate that the space-time location of the peak response also depends weakly on x/c_∞, however it is always found in the region $\theta < \frac{1}{\sqrt{\gamma}}$.

Although we have not been able to approximate the response shape for θ values larger than those corresponding to the arrival of the peak response at a given depth, we have investigated this region numerically by evaluating (1.17) with Mathematica. Figure 1.9 shows our results for $0.5 \leq \alpha \leq 0.9$; the vertical arrow indicates the arrival of the peak of the main response in the case $\alpha = 1$ (Debye model).

1.1.4. Summary. We have determined the small- and large-depth asymptotics of the impulse response of the Cole-Cole dielectric medium model. Our results were validated with independent numerical solutions of the full problem. The theoretical wavefront (short-depth) and large-depth responses of the Debye and Cole-Cole models are sufficiently distinct from each other so as to allow propagated pulse measurements in TDR setups to distinguish between the two. Significantly, our work shows that the measured wavefront response and the measured arrival of the main-response peak can be used to decide which dielectric permittivity model is most appropriate for a given set of exerimentally-obtained permittivity data. In closing we note that the asymptotic analysis of (1.17) for $\theta \geq \frac{c_\infty}{c_0}$ remains an open problem which must be solved first in order to obtain a uniform asymptotic approximation of the impulse response for $1 < \theta < \infty$.

1.2. Summary of Research Results to be Published.

1.2.1. The failure of the saddle-point method. The asymptotic analysis of (1.17) was shown above to be accurate for $1 \leq \theta < \frac{c_\infty}{c_0}$ and to break down for $\theta \to \frac{c_\infty}{c_0}$ from below, where c_∞ is the wavefront speed and c_0 is the zero-frequency phase speed. We have been able to determine the asymptotic form of

$$E(x,t) = \frac{1}{2\pi i}\int_{\zeta - i\infty}^{\zeta + i\infty} F(s) e^{s[t - \frac{x}{c_\infty}\sqrt{\frac{s^\alpha+\beta}{s^\alpha+\gamma}}]} ds, \quad t \geq \frac{x}{c_\infty}, \tag{1.22}$$

for $\theta > \frac{c_\infty}{c_0}$. The expression we obtained is as follows:

$$E(x,t) = \frac{\Delta}{\pi}\frac{\Gamma(\alpha+1)}{x(\theta - \sqrt{\frac{\beta}{\gamma}})^{\alpha+1}} Im\{e^{i\alpha\pi} F(\frac{\alpha+1}{x(\theta-\sqrt{\frac{\beta}{\gamma}})}, \alpha)\}, \tag{1.23}$$

where

$$\Delta = \frac{1}{2}\sqrt{\frac{\beta}{\gamma}}(\frac{1}{\beta} - \frac{1}{\gamma}),$$

and

$$F(r,\alpha) = \frac{e^{rx(\sqrt{\frac{r^\alpha e^{i\alpha\pi}+\beta}{r^\alpha e^{i\alpha\pi}+\gamma}} - \sqrt{\frac{\beta}{\gamma}})} - 1}{r\Delta e^{i\alpha\pi}}$$

We are presently attempting to verify (1.23) by comparing with numerical simulations obtained with the method described below and to fill the gap in the analysis for $\theta = \frac{c_\infty}{c_0}$.

1.2.2. Numerical methods for fractional differential equations. To incorporate, e.g., the Cole-Cole model in the FD-TD scheme we must be able to numerically solve the following fractional differential equation initial value problem for $\mathbf{P}$

$$\tau^\alpha \frac{d^\alpha \mathbf{P}}{dt^\alpha} + \mathbf{P} = (\epsilon_s - \epsilon_\infty)\mathbf{E}; \; t > 0, \; \mathbf{P}(0) = 0$$

where

$$\frac{d^\alpha \mathbf{P}}{dt^\alpha} = \frac{1}{\Gamma(1-\alpha)}\int_0^t \frac{\mathbf{P}'(\ell)}{(t-\ell)^\alpha} d\ell$$

is the Caputo fractional derivative of order $\alpha \in (0,1)$. We use

$$\Gamma(\alpha) = \int_0^\infty e^{-z} z^{\alpha-1} dz \text{ and } \Gamma(\alpha)\Gamma(1-\alpha) = \frac{\pi}{\sin \pi\alpha}$$

and a simple change of variables, $z = \xi^2(t-\ell)$, in the Caputo derivative to show:

$$\frac{d^\alpha \mathbf{P}}{dt^\alpha} = \frac{2\sin\pi\alpha}{\pi}\int_0^\infty \psi(\xi,t)d\xi, \; t > 0$$

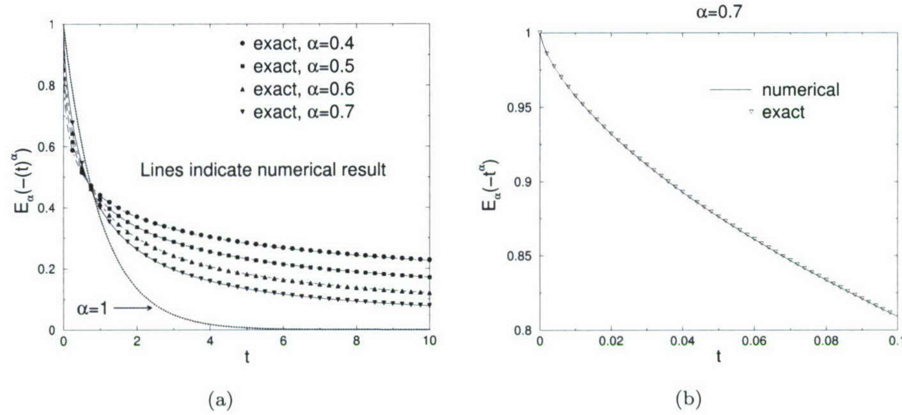

FIG. 1.10. *(a) Demonstration of accuracy of scheme to compute fractional derivatives; (b) demonstration of accuracy obtained with the scheme near $t = 0$.*

where $\psi(\xi, t)$ satisfies a non-homogeneous ordinary differential equation initial value problem

$$\frac{d\psi}{dt} + \xi^2\psi = \xi^{2\alpha-1}\frac{d\mathbf{P}}{dt}; \ t > 0, \ \psi(\xi, 0) = 0; \ 0 \leq \xi < \infty.$$

For accurate results we decompose $\int_0^\infty d\xi = \int_0^1 d\xi + \int_1^\infty$ and use the small$-\xi$ behavior $\psi(\xi, t) \sim y^{2\alpha-1}\mathbf{P}(t)$ and the large$-\xi$ behavior $\psi(\xi, t) \sim y^{2\alpha-3}\mathbf{P}'(t)$, determined from the above differential equation, along with Gaussian and Laguerre integration respectivelly. The discretization in ξ is then followed by a discretization in t using the trapezoidal rule; the result is an $O(\Delta t^2)$ accurate system of $N_g + N_l + 1$ equations that must be solved along with the FD-TD scheme. Typically, $N_g = N_l = 10 - 15$. The validation of the approach is shown in Figure 1.10 where the solution of the fractional ordinary differential equation

$$\frac{d^\alpha \mathbf{P}}{dt^\alpha} + \mathbf{P} = 0, \ \ \mathbf{P}(0^+) = 1,$$

is compared to the exact solution

$$\mathbf{P}(t) = E_\alpha(-t^\alpha), \ \ t > 0.$$

This work is in review [20].

1.2.3. The Cole-Davidson and Havriliak-Negami dielectric models. Previously, we found that the Debye, $\epsilon_D(\omega) = \epsilon_\infty + \frac{\epsilon_s - \epsilon_\infty}{1+i\omega\tau}$, wavefront impulse response supports discontinuities on $x = c_\infty t$, where $c_\infty = 1/\sqrt{\epsilon(\infty)\mu_0}$ is the wavefront speed, and that it decays exponentially with depth hence it is important only up to a distance of $O(c_\infty \tau)$ past the air/dielectric interface (the so-called "time-domain skin-depth"). Also, we found that past that thin layer the impulse response satisfies an advection-diffusion equation, that it travels with the zero-frequency phase speed along the sub-characteristic $x = \frac{c_\infty}{\sqrt{\epsilon_s}}t = c_0 t$, where $\epsilon_s = \epsilon(0)$ is the DC permittivity, and that it diffuses around that sub-characteristic. The Cole-Cole model's impulse response is infinitely smooth at the wavefront (small-depth). This is in contrast to the case of the Debye impulse response which is discontinuous at the wavefront. Also, the location of the peak of the main (large-depth) response occurs at an earlier space-time location than that found for the Debye dielectric model main response. Hence, the short-depth and large-depth responses of the Debye and Cole-Cole models are sufficiently distinct from each other so as to allow propagated pulse measurements in TDR setups to distinguish between the two when used to numerically model such experiments by fitting the two models to the same, experimentally determined, dielectric permittivity data.

For this reason we decided to extend the work done on the Cole-Cole dielectric model in order to investigate the remaining dielectric models of anomalous dispersion, namely the Cole-Davidson and Havriliak-Negami models. The Maxwell system in these dielectrics takes the following form

$$\mathbf{D}_t = \nabla \times \mathbf{H}, \quad \mu_0 \mathbf{H}_t = -\nabla \times \mathbf{E}$$

and is closed with the time-domain contitutive law

$$\mathbf{D}(t) = \epsilon_\infty \mathbf{E}(t) + \int_0^t \chi(t-t^{'})\mathbf{E}(t^{'})dt^{'}$$

where ($\alpha \in (0,1)$, $\beta \in (0,1)$)

$$\chi(t) = \chi^{CC}(t) = \mathcal{L}^{-1}(\frac{\epsilon_s - \epsilon_\infty}{1+(s\tau)^\alpha}), \ t > 0$$

<u>or</u>

$$\chi(t) = \chi^{CD}(t) = \mathcal{L}^{-1}(\frac{\epsilon_s - \epsilon_\infty}{(1+s\tau)^\beta}), \ t > 0$$

<u>or</u>

$$\chi(t) = \chi^{HN}(t) = \mathcal{L}^{-1}(\frac{\epsilon_s - \epsilon_\infty}{(1+(s\tau)^\alpha)^\beta}), \ t > 0$$

<u>or</u>

$$\chi(t) = \chi^{D}(t) = \mathcal{L}^{-1}(\frac{\epsilon_s - \epsilon_\infty}{1+s\tau}), \ t > 0.$$

Therefore we undertook to examine wave propagation (and develop numerical schemes to solve for the propagation of EM signals) in the following models:

- $\epsilon_{CC}(\omega) = \epsilon_\infty + \frac{\epsilon_s - \epsilon_\infty}{1+(i\omega\tau)^\alpha}$, $0 < \alpha < 1$, was proposed by Cole & Cole (J. Chem. Phys., v. 9, 1941) as an alternative to the Debye model ($\alpha = 1$).
- $\epsilon_{CD}(\omega) = \epsilon_\infty + \frac{\epsilon_s - \epsilon_\infty}{(1+i\omega\tau)^\beta}$, $0 < \beta < 1$, was proposed as an alternative to the above model by Davidson & Cole (J. Chem. Phys., v. 19, 1951) in order to have a model that resembles the Debye medium in the low-frequency limit while providing for a distribution of relaxation times.
- $\epsilon_{HN}(\omega) = \epsilon_\infty + \frac{\epsilon_s - \epsilon_\infty}{(1+(i\omega\tau)^\alpha)^\beta}$, $0 < \alpha < 1$, $0 < \beta < 1$, was proposed by Havriliak & Negami (J. Polym. Sci., v. 14, 1966) to combine the features in the above two models.

Alternatively, the constitutive law above can be implemented via writing

$$\mathbf{D}(t) = \epsilon_\infty \mathbf{E}(t) + \mathbf{P}(t)$$

where $\mathbf{P}(t)$ ($\mathbf{P}(0) = 0$) satisfies a fractional differential equation that involves

$$\frac{d^\alpha \mathbf{P}}{dt^\alpha} = \frac{1}{\Gamma(1-\alpha)} \int_0^t \frac{\mathbf{P}^{'}(\ell)}{(t-\ell)^\alpha} d\ell$$

which is the Caputo fractional derivative of order $\alpha \in (0,1)$. For numerical purposes one has to numerically solve fractional differential equations.

First, some results for the Cole-Cole Susceptibility obtained in our previous work. A representation of the Cole-Cole susceptibility is

$$\chi^{CC}(t) = \Delta \sum_{n=1}^{\infty} (-1)^{n+1} \frac{(t/\tau)^{n\alpha-1}}{\Gamma(n\alpha)}, \ t > 0$$

which, by referring to textbooks, can be written as

$$\chi^{CC}(t) = -\tau \Delta \frac{d}{dt} E_\alpha(-(t/\tau)^\alpha), \ t > 0$$

where $E_\alpha(z) = \sum_{n=0}^{\infty} \frac{z^n}{\Gamma(1+n\alpha)}$ is the Mittag-Leffler function of order α. For example, using a table of transforms, when $\alpha = 1/2$

$$\chi^{CC}(t) = \Delta[\frac{1}{\sqrt{\pi t/\tau}} - e^{t/\tau} erfc(\sqrt{t/\tau})], \quad t > 0$$

Given α, t, and τ one finds that $O(\frac{t/\tau}{\alpha})$ terms must be summed in order to evaluate $\chi_\alpha(t)$ and perform the convolution numerically in a wave propagation code. In addition, for $0 < \alpha < 1$, we have

$$\chi^{CC}(t) \sim O(\frac{1}{t^{1-\alpha}}), \quad t \to 0^+$$

$$\chi^{CC}(t) \sim O(\frac{1}{t^{1+\alpha}}), \quad t \to \infty$$

Thus, $\chi^{CC}(t) \in L^p$ for $1 \leq p < \frac{1}{1-\alpha}$ thus *only* for $\alpha > 1/2$ does $\chi_\alpha(t)$ belong to the intersection of L^1 and L^2, i.e., the Fourier transform (and the Kramers-Kronig relations) require more care for $\alpha \leq 1/2$ since then $\chi^{CC}(t)$ is only in L^1. In biological and geophysical applications $0.6 \leq \alpha \leq 0.9$.

Next, we give some results for the Cole-Davidson Susceptibility model. For the Cole-Davidson dielectric, the time-domain susceptibility is ($\beta \to 1^-$ is the Debye model)

$$\chi^{CD}(t) = \mathcal{L}^{-1}(\frac{\epsilon_s - \epsilon_\infty}{(1+s\tau)^\beta}) = \frac{\epsilon_s - \epsilon_\infty}{\tau^\beta} \frac{t^{\beta-1}}{\Gamma(\beta)} e^{-t/\tau}, \ t > 0$$

which can be used to determine the polarization ODE

$$(\frac{d}{dt} + \frac{1}{\tau})^\beta \mathbf{P} = e^{-t/\tau} \frac{d^\beta}{dt^\beta}[e^{t/\tau}\mathbf{P}] = \frac{\epsilon_s - \epsilon_\infty}{\tau^\beta} \mathbf{E}; \ t > 0, \ \ \mathbf{P}(0) = 0$$

for use in the constitutive law

$$\mathbf{D}(t) = \epsilon_\infty \mathbf{E}(t) + \mathbf{P}(t)$$

where $\frac{d^\beta}{dt^\beta}$ is again the Caputo fractional derivative of order $\beta \in (0,1)$. The Cole-Davidson fractional differential equation was obtained through use of the following Laplace transform identity

$$\mathcal{L}\{(\frac{d}{dt} + \gamma)^\beta f(t)\}(s) = \mathcal{L}\{e^{-\gamma t} \frac{d^\beta}{dt^\beta}(e^{\gamma t} f(t))\}(s) =$$

$$\mathcal{L}\{\frac{d^\beta}{dt^\beta}(e^{\gamma t} f(t))\}(s+\gamma) = (s+\gamma)^\beta \mathcal{L}\{e^{\gamma t} f(t)\}(s+\gamma) - f(0^+)(s+\gamma)^{\beta-1} =$$

$$(s+\gamma)^{\beta}F(s),$$

since our initial condition on the polarization requires $f(0^+) = 0$, and the following relation

$$\mathbf{P}(s) = \frac{\epsilon_s - \epsilon_\infty}{\tau^\beta}\frac{\mathbf{E}(s)}{(1+s\tau)^\beta}$$

for the polarization in the frequency domain. Numerically, the Cole-Davidson model would employ the following

$$\frac{d^\beta}{dt^\beta}[e^{t/\tau}\mathbf{P}] = \frac{2\sin\pi\beta}{\pi}\int_0^\infty \psi^{CD}(\xi,t)d\xi,\ t>0,$$

where $\psi^{CD}(\xi,t)$ satisfies a non-homogeneous ordinary differential equation initial value problem

$$\frac{d\psi^{CD}}{dt} + \xi^2\psi^{CD} = \xi^{2\beta-1}(\frac{d\mathbf{P}}{dt} + \frac{1}{\tau}\mathbf{P})e^{t/\tau};\ t>0,$$

subject to the initial condition

$$\psi^{CD}(\xi,0) = 0;\ 0 \le \xi < \infty$$

in order to solve

$$\frac{d^\beta}{dt^\beta}[e^{t/\tau}\mathbf{P}] = \frac{\epsilon_s - \epsilon_\infty}{\tau^\beta}\mathbf{E}e^{t/\tau};\ t>0,\quad \mathbf{P}(0)=0$$

In order to tackle the Havriliak-Negami model we need the following:

$$(s+\frac{1}{\tau})^\beta = \sum_{k=0}^{\infty}\frac{1}{\tau^k}\frac{(-1)^k\Gamma(k-\beta)}{\Gamma(1+k)\Gamma(-\beta)}s^{\beta-k}$$

so that the application of the inverse Laplace transform to both sides gives

$$(\frac{d}{dt}+\frac{1}{\tau})^\beta = \sum_{k=0}^{\infty}\frac{1}{\tau^k}\frac{(-1)^k\Gamma(k-\beta)}{\Gamma(1+k)\Gamma(-\beta)}(\frac{d}{dt})^{\beta-k}$$

Then we can solve the fractional differential equation ($H(t)$ is the Heavyside step function)

$$(\frac{d}{dt}+\frac{1}{\tau})^\beta\mathbf{P}(t) = \frac{\Delta}{\tau^\beta}H(t)$$

using the Laplace transform and subsequently obtain the Green's function, $\frac{d\mathbf{P}(t)}{dt}$, for solving it with a general right-hand side, i.e.,

$$\frac{\Delta}{\tau}\sum_{k=0}^{\infty}\frac{(-1)^{k+1}(\beta+k)\Gamma(\beta+k)}{\Gamma(\beta)\Gamma(k+1)\Gamma(1+\beta+k)}(\frac{t}{\tau})^{\beta+k-1} =$$

$$= \chi^{CD}(t) = \frac{\Delta}{\tau}\sum_{k=0}^{\infty}\frac{(-1)^{k+1}}{\Gamma(\beta)\Gamma(k+1)}(\frac{t}{\tau})^{\beta+k-1}$$

which is just an alternative representation of $\frac{\Delta}{\tau^\beta}\frac{t^{\beta-1}}{\Gamma(\beta)}e^{-t/\tau}$. Clearly,

$$\chi^{CD}(t) \sim O(\frac{1}{t^{1-\beta}}),\quad t\to 0^+$$

$$\chi^{CD}(t) \sim O(e^{-t/\tau}), \quad t \to \infty$$

So the CD model resembles the CC at short times and the Debye at long times. In the above derivation we used $\frac{d^q}{dt^q}H(t) = \frac{t^{-q}}{\Gamma(1-q)}$.

Finally, we give results obtained for the Havriliak-Negami susceptibility function. To find the Green's function for the fractional differential equation which will be coupled to Maxwell's equations we use

$$(s^\alpha + \frac{1}{\tau^\alpha})^{-\beta} = \sum_{k=0}^{\infty} \frac{1}{\tau^{k\alpha}} \frac{(-1)^k \Gamma(k+\beta)}{\Gamma(1+k)\Gamma(\beta)} s^{-\alpha(\beta+k)},$$

and the property $\frac{d^q}{dt^q}H(t) = \frac{t^{-q}}{\Gamma(1-q)}$, to first solve

$$(\frac{d^\alpha}{dt^\alpha} + \frac{1}{\tau^\alpha})^\beta \mathbf{P}(t) = \frac{\Delta}{\tau^{\alpha\beta}} H(t)$$

i.e.

$$\mathbf{P}(t) = \Delta \sum_{k=0}^{\infty} \frac{(-1)^{k+1}\Gamma(\beta+k)}{\Gamma(\beta)\Gamma(k+1)\Gamma(1+\alpha(\beta+k)} (\frac{t}{\tau})^{\alpha(\beta+k)}.$$

Subsequent time differentiation gives

$$\chi^{HN}(t) = \frac{\Delta}{\tau} \sum_{k=0}^{\infty} \frac{(-1)^{k+1}\Gamma(\beta+k)}{\Gamma(\beta)\Gamma(k+1)\Gamma(\alpha(\beta+k)} (\frac{t}{\tau})^{\alpha(\beta+k)-1}$$

The asymptotic behavior now is

$$\chi^{HN}(t) \sim O(\frac{1}{t^{1-\alpha\beta}}), \quad t \to 0^+$$

$$\chi^{HN}(t) \sim O(\frac{1}{t^{1+\alpha}}), \quad t \to \infty$$

So the HN model resembles the CC at short times (but with slower decay) and at long times (identical decay). For the non-dimensionalized signaling problem in a Havriliak-Negami dielectric half space ($x \geq 0$) the electric field is given by the following Bromwich integral ($E = 0, \ t < x$)

$$E(x,t) = \frac{1}{2\pi i} \int_{\zeta - i\infty}^{\zeta + i\infty} F(s) e^{s[t - x\sqrt{1 + \frac{\gamma}{(s^\alpha + \delta^\alpha)^\beta}}]} ds, \quad t \geq x$$

where $-\pi < arg(s) \leq \pi$, $Re\sqrt{\cdot} > 0$, $\gamma = (\frac{T_p}{\tau})^{\alpha\beta}(\frac{\epsilon_s}{\epsilon_\infty} - 1)$, $\delta = \frac{T_p}{\tau}$, and $F(s)$ is the Laplace transform of the time-domain signaling data imposed at $x = 0$. For the branch chosen, the SQRT does not introduce additional singularities (recall, $0 < \alpha < 1$ & $0 < \beta < 1$). We first want to know the $t \to x^+$ behavior of the response with $F(s) = 1$, i.e., the wavefront behavior of the HN Green's function. The large$-s$ expansion

$$t - x + x(1 - \sqrt{1 + \frac{\gamma}{(s^\alpha + \delta^\alpha)^\beta}}) = (t - x) - x\frac{\gamma}{2} s^{-\alpha\beta} + O(xs^{-\alpha(1+\beta)})$$

gives

$$E(x,t) \approx \frac{1}{2\pi i} \int_{\zeta - i\infty}^{\zeta + i\infty} F(s) e^{-As^{1-\alpha\beta}} e^{s(t-x)} ds,$$

where $A = x\frac{\gamma}{2} > 0$. Since $1 - \alpha\beta > 0,\ \gamma > 0$, we find

$$\lim_{t \to x^+} \frac{d^n}{dt^n} E(x,t) = 0,\ n \geq 0,$$

since

$$\lim_{s \to \infty} s^n F(s) e^{-As^{1-\alpha\beta}} = 0,\ n \geq 0.$$

Thus, the response of the Havriliak-Negami medium is infinitely smooth at the wavefront even in the case of $F(s) = 1$ ($f(t) = \delta(t)$ signaling data). This is similar to the Cole-Cole dielectric. In contrast, for the Debye model ($\alpha = 1,\ \beta = 1$) we obtain

$$E(x,t) \approx e^{-\frac{x}{2c_\infty \tau}(\frac{\epsilon_s}{\epsilon_\infty} - 1)} f(t - \frac{x}{c_\infty}),$$

i.e., the Debye wavefront response inherits the continuity properties of $f(t)$ at $t = 0$ and decays exponentially fast thus exhibiting a "time-domain skin-depth" (see TMR & PGP, *JOSA-A* (1996), and PGP, *WAVE MOTION* (1995)). Integrating $\mathcal{L}^{-1}\{e^{-s^{1-\alpha\beta}}\}$ around the branch cut we obtain the wavefront response for any $\alpha,\ \beta$ in terms of the function

$$\Psi_{\alpha,\beta}(T) = \frac{1}{\pi} \int_0^\infty e^{-Tr} e^{-r^{1-\alpha\beta} \cos[\pi(1-\alpha\beta)]} \sin(r^{1-\alpha\beta} \sin[\pi(1-\alpha\beta)]) dr,$$

$T > 0$, where $T = t - x$. NOTE: $\lim_{\alpha,\ \beta \to 1^-} \Psi_{\alpha,\beta}(T) = e^{-1}\delta(T)$. Then, the translation theorem allows us to write an integral expression for the approximate wavefront response for any $0 < \alpha < 1,\ 0 < \beta < 1$ as a convolution of $f(t)$ with the approximate impulse response function

$$\mathcal{I}^{app}(x,t) = \mathcal{L}^{-1}\{e^{-As^{1-\alpha\beta}}\} = A^{-\frac{1}{1-\alpha\beta}} \Psi_{\alpha,\beta}(A^{-\frac{1}{1-\alpha\beta}}(t - x)),\quad t \geq x.$$

A publication that compares and contrasts these various dielectric models from the point of view of their respective EM pulse responses is in preparation.

REFERENCES

[1] Petropoulos P.G., *On the Time-Domain Response of Cole-Cole Dielectrics*, IEEE Transactions on Antennas and Propagation, vol. 53 (2005), pp. 3741-3746.

[2] Carin L., Sichina J. and Harvey J. F., *Microwave Underground Propagation and Detection*, IEEE Transactions on Microwave Theory and Techniques, 50 (2002), pp. 945-952.

[3] Polk C. and Postow E. (eds.), *Handbook of Biological Effects of Electromagnetics Fields*, Boca Raton: CRC Press LLC (1995).

[4] Bertolini D., Cassettari M., Salvetti G., Tombari E. and Veronesi S., *Time Domain Reflectometry to Study the Dielectric Properties of Liquids: Some Problems and Solutions*, Review of Scientific Instruments, 62 (1991), pp. 450-456.

[5] Farr E.G. and Frost C.A., *Impulse Propagation Measurements of Water, Dry Sand, Moist Sand, and Concrete*, US Air Force Weapons Laboratory Technical Report WL-TR-1997-7051. Available: http://handle.dtic.mil/100.2/ADA328785.

[6] Roberts T.M., *Measured and Predicted Behavior of Pulses in Debye- and Lorentz-Type Materials*, IEEE Transactions on Antennas and Propagation, 52 (2004), pp. 310-314.

[7] Debye P., *Polar Molecules*, Chemical Catalogue Company, New York (1929).

[8] Cole K.S. and Cole R.H., *Dispersion and Absorption in Dielectrics*, Journal of Chemical Physics, 9 (1941), pp. 341-351.

[9] Hurt W.D., *Multiterm Debye Dispersion-Relations for Permittivity of Muscle*, IEEE Transactions on Biomedical Engineering, 32 (1985), pp. 60-64.

[10] Gabriel C., *Compilation of the Dielectric Properties of Body Tissues at RF and Microwave Frequencies*, Technical Report AL/OE-TR-1996-0037, USAF Armstrong Laboratory, Brooks AFB, TX (1996).

[11] Robert A., *Dielectric Permittivity of Concrete Between 50 Mhz and 1 Ghz and GPR Measurements for Building Materials Evaluation*, Journal of Applied Geophysics, 40 (1998), pp. 89-94.

[12] Petropoulos P.G., *The Wave Hierarchy for Propagation in Relaxing Dielectrics*, Wave Motion, 21 (1995), pp. 253-262.

[13] Roberts T.M. and Petropoulos P.G., *Asymptotics and Energy Estimates for Electromagnetic Pulses in Dispersive Media*, Journal of the Optical Society of America A, 13 (1996), pp. 1204-1217.

[14] Roberts T.M. and Petropoulos P.G., *Asymptotics and Energy Estimates for Electromagnetic Pulses in Dispersive Media: Addendum*, Journal of the Optical Society of America A, 16 (1999), pp. 2799-2800.

[15] Bottcher C.J.F. and Bordewijk P., *Theory of Electric Polarization, Vol. II*, Elsevier Scientific Publishing Company, New York (1978).

[16] Van Gemert M.J.C., *A Note on the Cole-Cole Dielectric Permittivity Equation in Connection with Causality*, Chemical Physics Letters, 14 (1972), pp. 606-608.

[17] Jackson J.D., *Classical Electrodynamics, 2nd Ed*, Wiley, New York (1975).

[18] Oldham K.B. and Spanier J., *The Fractional Calculus*, Academic Press, New York (1974).

[19] Pollard H., *The Representation of* e^{-x^λ} *as a Laplace Integral*, Bulletin of the American Mathematical Society, 52 (1946), pp. 908-910.

[20] Petropoulos P.G., *A Numerical Scheme for the Solution of the Time-Dependent Maxwell Equations in Dielectrics Exhibiting Fractional Relaxation of the Induced Polarization*, in review (2006).